East Asian Journal on Applied Mathematics
doi: 10.4208/eajam.050911.300112a

Vol. **2**, No. 1, pp. 47-58
February 2012

Longshore Submerged Wave Breaker for a Reflecting Beach

S. R. Pudjaprasetya[1,*] and Elis Khatizah[2]

[1] *Industrial and Financial Mathematics Research Group, Faculty of Mathematics and Natural Sciences, Institut Teknologi Bandung, Jalan Ganesha 10, Bandung, Indonesia, 40132.*
[2] *Mathematics Department, Bogor Agricultural University, Indonesia.*

Received 5 September 2011; Accepted (in revised version) 30 January 2012

Available online 10 February 2012

Abstract. This paper considers the effect of a hard-wall beach on the downstream side of submerged parallel bars in a breakwater. In previous research, it was assumed that the beach can absorb all of the transmitted wave energy, when an optimal dimension for a submerged parallel bar is obtained and the wave amplitude is reduced as more bars are installed. However, for a hard-wall beach there are waves reflected from the beach that change the long-term wave interaction. We adopt the linear shallow water equations in Riemann invariant form and use the method of characteristics, in a procedure applicable to various formations of submerged rectangular bars. The distance from the parallel bar (or bars) to the beach determines the phase differences between right running waves in the beach basin and whether they superpose destructively or constructively before hitting the beach, to define the safest and the most dangerous cases. Our numerical calculations for one bar, two bars and for periodic rectangular bars confirm the analytical formulae obtained.

AMS subject classifications: 65M25, 74J20, 35L05
Key words: Method of characteristics, submerged parallel wave bars, shallow water equations.

1. Introduction

Whenever an incoming water wave enters a region where the depth suddenly changes, it scatters into a transmitted wave and a reflected wave. This mechanism underlies the concept of wave breakers, which scatter incoming waves so their amplitudes are reduced. Breakwaters consisting of submerged solid bars are often used. In Mei *et al.* [1], the optimal dimension of the one-bar submerged breakwater was determined. In Pudjaprasetya *et al.* [2], the optimal dimension of the submerged breakwater was simulated and a generalisation to consider an n-bar submerged breakwater was discussed. Wiryanto [3] studied

*Corresponding author. *Email addresses:* `sr_pudjap@math.itb.ac.id` (S. R. Pudjaprasetya), `elis.kh@gmail.com` (E. Khatizah)

wave propagation over a submerged bar by solving an appropriate linear potential problem, and his results clearly indicated there is an optimal dimension for the submerged bar. Mattioli [4] studied resonant reflection due to a series of submerged solid bars, and in particular the effect of evanescent modes. In all of this work, it is assumed that the beach can absorb all of the transmitted wave energy.

Incident waves are also scattered by another type of breakwater, the sinusoidal submerged bar. A sinusoidal bar can be a very effective scatterer due to Bragg resonance — cf. Heathershaw [5] for experimental work, and Davies & Heathershaw [6] for theory — cf. also [1]. Indeed, a rather small sinusoidal breakwater amplitude may produce a quite large reflected wave amplitude, and hence a transmitted wave of correspondingly small amplitude. Bragg resonance occurs when the incident wavelength is nearly twice the wavelength of the sinusoidal bars. Yu and Mei [7] studied the effect of shore reflection from a vertical wall, located at some distance to the right of the sinusoidal breakwater. They found that the free-surface oscillations at the wall can vary between 1 to 3.6 times the amplitude of the incident waves, depending on the distance between the breakwater and the wall.

For practical reasons, the bars in a man-made breakwater are very simple, such as rectangular. However, the case of a sinusoidal breakwater indicates the effect of shore reflection downstream from the breakwater should be studied thoroughly before construction. In this paper, we use the linear shallow water equation in Riemann invariant form to consider a monochromatic wave incident on a piecewise constant bottom topography with a reflecting (hard-wall) beach, and study the interaction between the reflected and transmitted waves. The distance between the breakwater and the beach is found to define the phase difference between the right running waves in the beach basin, and hence whether these waves superpose destructively or constructively. For a breakwater consisting of parallel rectangular bars with an optimal dimension, a formula for the safest and the most dangerous distances can be obtained. We solve the shallow water equation for the piecewise constant bottom topography numerically, using the method of characteristics. In this way, we are able to impose an incident right running monochromatic wave and simultaneously absorb the left running reflected wave, and eventually observe the long-term wave interaction. For a one-bar breakwater of a certain height, the wave amplitude in the beach basin is found to vary between 1.26 to 3.12 times the incident wave amplitude depending on the distance between the breakwater and the wall, similar to the result found for the sinusoidal submerged bar [7]. The distance between the reflecting wall and the submerged bar is therefore key to the qualitative change of the wave response. Although linear, this work provides important insight into the effect of a reflecting boundary, and may also be applicable in acoustics and optics. The analogy between water waves and optics is discussed in Andonowati & Van Groesen [8], and in Gisolf & Verschuur [9] for acoustic waves.

For clarity, let us here briefly reconsider the optimal dimension of a submerged bar. When an incident monochromatic wave with amplitude A passes a submerged bar of a certain height and width, due to reflections at the depth change the wave scatters into a transmitted wave with amplitude A_T and a reflected wave with amplitude A_R. The value of A_T/A depends on the height and width of the bar, but a greater bar width does not directly make A_T/A smaller and this quotient depends periodically on the bar width. The optimal width of a bar with a certain height is the smallest width that minimises A_T/A. If we assume that the fluid layer above the bar has depth h_i, the optimal width of the bar L_i is given by

$$2k_i L_i = \pi\,, \tag{1.1}$$

where k_i is the local wavelength in the dispersion relation $\omega/k_i = \sqrt{gh_i}$ (with ω the wave frequency and g the gravitational constant). The explicit formula for L_i in terms of h_i and ω is thus

$$L_i = \frac{\pi}{2}\frac{\sqrt{gh_i}}{\omega}\,, \tag{1.2}$$

so that for a specific wave frequency ω the optimal width only varies with the water depth above the bar h_i.

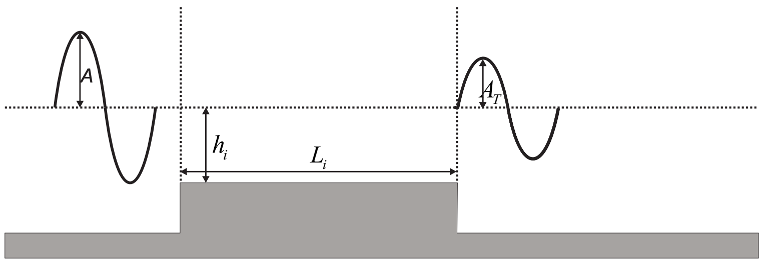

Figure 1: Diagram of a one-bar wave reflector, with depth h_i and optimal width L_i.

2. Method of Characteristics

In this section, we formulate the method of characteristics for the shallow water equation given a piecewise constant depth. For a surface elevation $\eta(x,t)$ and horizontal flux $Q(x,t)$, the shallow water equations in Riemann invariant form are

$$\left(\partial_t - c\partial_x\right)(c\eta - Q) = 0, \tag{2.1}$$

$$\left(\partial_t + c\partial_x\right)(c\eta + Q) = 0, \tag{2.2}$$

where $c = \sqrt{gh}$. Introducing characteristic variables $\xi(x,t) = x + ct$ and $\psi(x,t) = x - ct$, Eqs. (2.1) and (2.2) become

$$\partial_\psi(c\eta - Q) = 0, \qquad \partial_\xi(c\eta + Q) = 0\,,$$

with solution $c\eta - Q = f(\xi)$ and $c\eta + Q = g(\psi)$ where f and g are arbitrary functions. Hence $c\eta - Q$ is constant along the characteristic $\xi = x + ct =$ constant, and $c\eta + Q$ is constant along the characteristic $\psi = x - ct =$ constant.

Let us now consider the case of one submerged bar with height $(h_2 - h_1)$ and width L_2 on a flat bottom with depth h_1, so the depth is given by

$$h(x) = \begin{cases} h_2 \,, & 0 < x < L_2, \\ h_1 \,, & x < 0 \text{ or } x > L_2 \,. \end{cases} \tag{2.3}$$

We consider the space-time domain $\left[a, X_{total}\right] \times [0, T]$ with $a < 0 < L_2 < X_{total}$, and apply the method of characteristics. The time domain is discretised uniformly with increments $\triangle t$, whereas the partition in the spatial domain depends on the depth — i.e. we take the step sizes

$$\triangle x_i = \sqrt{g h_i}\, \triangle t \,, \tag{2.4}$$

where $i = 1, 2$. Thus the partition in the spatial domain is not homogenous, with Δx_1 on any interval where the depth is h_1 and Δx_2 on any interval where the depth is h_2. The discretised form of Eqs. (2.1) and (2.2) is thus

$$\begin{cases} c_L \eta_P + Q_P = c_L \eta_L + Q_L \,, \\ c_R \eta_P - Q_P = c_R \eta_R - Q_R \,, \end{cases} \tag{2.5}$$

where $c_L = \sqrt{g h(x_L)}$ with x_L the coordinate of grid point L, and similarly for c_R.

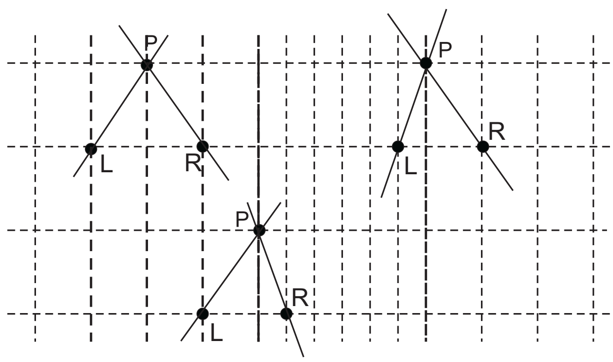

Figure 2: Grid point P for three different cases — viz. in the interior of a homogeneous grid, and at the interfaces between two different partitions.

By taking this inhomogeneous partition in the spatial domain, we can ensure that the grid points P and L always lie in the same rightward characteristic $\psi(x, t) = \text{constant}$, whereas the grid points P and R always lie in the same leftward characteristic $\xi(x, t) = \text{constant}$. Eqs. (2.5) hold for any grid point P in the domain $\left[a, X_{total}\right]$, including the points of depth discontinuity, and yield the explicit formulas

$$\begin{cases} Q_P = \left(c_R(c_L \eta_L + Q_L) - c_L(c_R \eta_R - Q_R)\right) / (c_L + c_R) \\ \eta_P = (c_R \eta_R - Q_R + Q_P)/c_R \end{cases} . \tag{2.6}$$

Moreover, for the long time simulation in the finite domain, we want to impose a rightward running monochromatic wave from the left boundary and at the same time allow a leftward running reflected wave to pass through. This can be done directly from Eqs. (2.5), because Riemann values are constant along the corresponding characteristics. Thus for points P along the left boundary $x = a$, Eqs. (2.5) hold with η_L and Q_L at ghost points for an incident rightward running monochromatic wave with amplitude A — i.e.

$$\eta_L = A\sin\omega t, \qquad Q_L = c_L\eta_L = c_L A\sin\omega t. \tag{2.7}$$

2.1. Phase differences at depth discontinuities

Let us now determine the phase differences between the reflected and transmitted waves compared to the incident wave, around depth discontinuities. We take as initial condition a sinusoidal incoming wave from the left

$$\eta(x,0) = \begin{cases} \sin(-k_1 x), & x < 0 \\ 0, & x \geq 0 \end{cases}, \qquad Q(x,0) = c_1\eta(x,0), \tag{2.8}$$

corresponding to the incoming wave field for $x < 0$

$$\eta(x,t) = \sin(\omega t - k_1 x), \tag{2.9}$$

$$Q(x,t) = c_1 \sin(\omega t - k_1 x) \tag{2.10}$$

with $\omega/k_1 = c_1$. Next, we take a closer look at the area around $x = 0$, the point of depth discontinuity. Fig. 3 shows four triangular sectors in the x, t-plane for $t > 0$, in each of which the propagation has a different character. The sector on the right of II is dead water, where both η and Q are zero. The sector on the left of I has the incoming wave. Our main interest is in Sectors I and II.

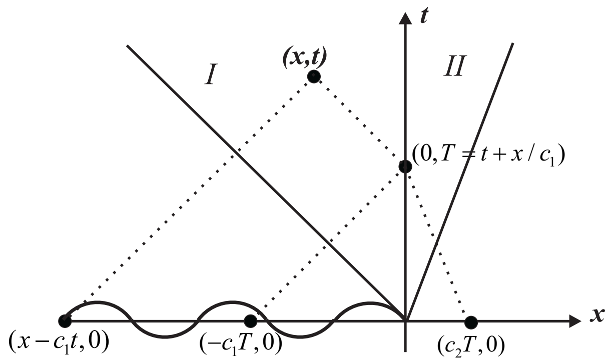

Figure 3: Characteristic lines that influence values of η and Q at a point (x,t) in Sector I.

First, we calculate the interface values η and Q, at the point $(0,T)$ in Fig. 3. These values are determined by the value of $c_1\eta + Q$ at $(-c_1T,0)$ and the value of $c_2\eta - Q$ at $(c_2T,0)$. The equations

$$\begin{cases} c_1\eta + Q|_{(0,T)} = (c_1\eta + Q)|_{(-c_1T,0)} = 2c_1\sin(-k_1x)|_{x=-c_1T} = 2c_1\sin(\omega T) \\ c_2\eta - Q|_{(0,T)} = (c_2\eta - Q)|_{(c_2T,0)} = 0 \end{cases}$$

yield

$$\eta(0,T) = \frac{c_1}{\tilde{c}} \sin \omega T \tag{2.11}$$

$$Q(0,T) = \frac{c_1 c_2}{\tilde{c}} \sin \omega T \tag{2.12}$$

with $\tilde{c} \equiv (c_1 + c_2)/2$. Next, we calculate η and Q at the point (x,t) in Sector I, determined from

$$\begin{cases} c_1\eta + Q|_{(x,t)} = c_1\eta + Q|_{(x-c_1t,0)} = 2c_1 \sin(\omega t - k_1 x) \\ c_1\eta - Q|_{(x,t)} = c_1\eta - Q|_{(0,T)} = c_1 \left(\dfrac{c_1 - c_2}{\tilde{c}}\right) \sin(\omega t + k_1 x) \end{cases} .$$

Thus we obtain

$$\eta(x,t) = \sin(\omega t - k_1 x) + \frac{c_1 - c_2}{c_1 + c_2} \sin(\omega t + k_1 x), \tag{2.13}$$

$$Q(x,t) = c_1 \sin(\omega t - k_1 x) - c_1 \frac{c_1 - c_2}{c_1 + c_2} \sin(\omega t + k_1 x), \tag{2.14}$$

respectively defining the rightward and leftward running waves. Analogously, in Sector II we find

$$\eta(x,t) = \frac{c_1}{\tilde{c}} \sin(\omega t - k_2 x), \tag{2.15}$$

$$Q(x,t) = \frac{c_1 c_2}{\tilde{c}} \sin(\omega t - k_2 x). \tag{2.16}$$

On comparing Eq. (2.15) with Eq. (2.9), we see the transmitted wave is just the interface profile propagated undisturbed along the characteristic, with the same phase as the incident wave. The solution in Sector II thus connects continuously to the interface data, as it should do. Moreover, in Eq. (2.15) there is a factor $c_1/\tilde{c}$, and in the discharge (2.16) there is a factor $c_2/\tilde{c}$. Thus when $c_2 < c_1$ (the wave arrives at a bottom upward step), the elevation factor is greater than 1 and the discharge factor is less than 1.

Next, let us consider Sector I. Comparing the reflected wave equations (2.13) and (2.9), we have a factor $(c_1 - c_2)/(c_1 + c_2)$. When $c_2 < c_1$ (the wave arrives at a bottom upward step), the elevation factor is positive such that the reflected wave has the same phase as the incident wave. On the other hand, when $c_2 > c_1$ (the wave arrives at a bottom downward step) the reflected wave has negative amplitude, so the phase of the reflected wave changes by π.

After passing a submerged bar, the wave goes further to the right. When it arrives at the hard wall $x = L_b$, the values of η and Q for $h_2 \to 0$ can be determined from Eqs. (2.11) and (2.12) — viz.

$$\eta(L_b,t) = 2\sin \omega t, \tag{2.17}$$

$$Q(L_b,t) = 0\,. \tag{2.18}$$

It is notable that Eqs. (2.13) to (2.18) hold for all time, because the Riemann value is constant along each corresponding characteristic irrespective of the features of any characteristics of the other family that it intersects. We simulate a monochromatic wave coming from the left, passing an area with submerged bars, and then going further right before hitting the hard wall. This process is to be observed for some time, in order to see the long term wave interaction behaviour. We implement the discretised equation (2.5) with the left influx boundary (2.7), the right hard wall boundary (2.17-2.18) and the still water level initial condition, using inhomogeneous spatial partitions that satisfy the Courant condition (2.4).

In summary, the phases of transmitted and reflected waves compared to the phase of the incident wave may be summarised as follows.

1. When a wave enters a bottom upward step, both the transmitted and reflected waves have the same phase as the incident wave.
2. When a wave enters a bottom downward step, the transmitted wave has the same phase as incident wave, but the phase of the reflected wave is changed by π.
3. When a wave hits a hard-wall beach, the reflected wave has the same phase as the incident wave.

This information will be used to determine the phase difference between successive right running waves before they hit the hard-wall beach to the right, as discussed in the next section.

3. Constructive or Destructive Interference

In this section, the effect of a hard-wall beach on wave-submerged bar interaction is investigated. By tracking phase differences between the waves, we can determine the safest hard-wall distance, corresponding to destructive wave interference.

Let us consider the one bar topography defined by Eq. (2.3), with the hard-wall beach on the right at distance L_b as shown in Fig. 4, and an incident rightward running monochromatic wave passing the submerged solid bar. Every time a wave passes, it splits into a reflected and a transmitted wave. Our main interest is the amplitude of right running waves in the beach basin, which is the area $L_2 < x < L_2 + L_b$. Thus in this area there are infinitely many right running waves resulting from repetitious scattering at $x = 0$ and at $x = L_2$, and we consider the superposition of those waves that hit the hard-wall beach. Their phase differences determine whether they superpose constructively or destructively.

Consider the phase difference between the first right running wave and the second, caused by scattering at $x = L_2$. Compared to the first, the second wave travels L_b further right, hit the hard-wall (with no change in phase), and then travels back to the left a distance L_b until it is scattered at $x = L_2$. The reflected wave caused by the bottom upward step at $x = L_2$ has no phase change, so the phase difference between these two successive waves is only due to the difference in distance travelled — viz.

$$\theta = 2k_1 L_b. \tag{3.1}$$

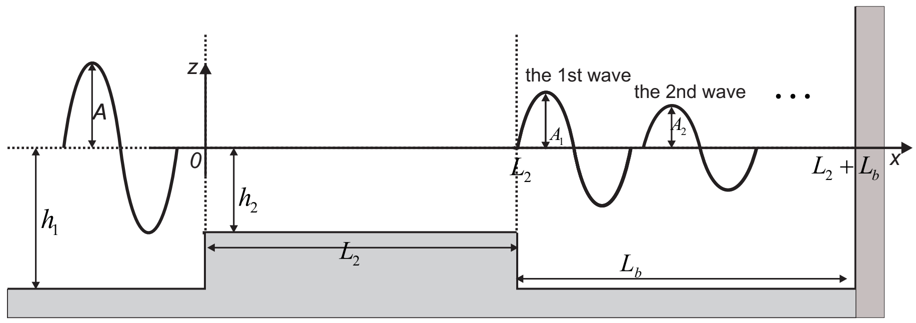

Figure 4: One submerged bar with optimal dimension and a hard-wall beach on the right at distance L_b.

Eq. (3.1) also gives the phase difference θ caused by scattering at $x = L_2$, for any other pair of successive right running waves.

Let us next consider the right running wave on the beach basin $L_2 < x < L_2 + L_b$ that results from scattering processes at $x = 0$. Compared to the first wave, the second travels a distance L_b further to the right, hits the hard-wall, and then travels back to the left a distance L_b until it meets a bottom upward step at $x = L_2$. The transmitted wave caused by scattering at the bottom upward step at $x = L_2$ has no change in phase, and it continues to travel L_2 further left until it meets the bottom downward step at $x = 0$. The phase of the reflected wave caused by the bottom downward step at $x = 0$ is changed by π, and it travels further to the right a distance L_2. Thus the phase difference between the first and second right running waves caused by the scattering at $x = 0$ is

$$\theta = 2k_1 L_b + 2k_2 L_2 + \pi = 2k_1 L_b \ ,$$

since the optimal width L_2 of the bar satisfies (1.1). Further, the phase difference between two successive right running waves on $L_2 < x < L_2 + L_b$ caused by scattering at $x = 0$ is also given by Eq. (3.1).

Consequently, at any time the amplitude of the right running wave on the beach basin $L_2 < x < L_2 + L_b$ can be expressed as

$$A_T = \Sigma_{m=0}^{\infty} A_m \exp(im\theta) \ ,$$

where A_m is the amplitude of the m-th monochromatic wave and θ is the phase difference between two successive monochromatic waves. Thus when $\theta = (2n+1)\pi$ where n is an integer, A_T is the infinite sum of the alternating series; and when $\theta = 2n\pi$ where n is an integer, A_T is the infinite sum of its positive series. Moreover, A_T has a minimum whenever $\theta = 2k_1 L_b = (2n+1)\pi$ or

$$L_b = \left(n + \frac{1}{2}\right)\frac{\pi}{k_1} = \left(n + \frac{1}{2}\right)\frac{\lambda_1}{2} = \left(n + \frac{1}{2}\right)\pi\frac{\sqrt{gh_1}}{\omega}, \tag{3.2}$$

and a maximum whenever

$$L_b = n\frac{\pi}{k_1} = n\frac{\lambda_1}{2} = n\pi\frac{\sqrt{gh_1}}{\omega}. \tag{3.3}$$

Consequently, we conclude that right running waves superpose destructively in the beach basin for the distance given by Eq. (3.2), but constructively for that given by Eq. (3.3). It is to be expected that similar analysis applies for other configurations of submerged bars with optimal dimensions.

3.1. Examples

We have considered several types of submerged solid breakwater by implementing the discretised shallow water equation (2.5) with the left influx boundary condition (2.7), right hard wall boundary conditions (2.17) and (2.18), and the still water level initial condition — viz. one-bar, two-bar and periodic bar, on a constant depth $h_1 = 10$ with submerged bars where $h_2 = 4$. For all computations, we considered an incident monochromatic wave with amplitude $A = 1$ and frequency $\omega = 1$, and approximated the gravitational constant as $g = 10$m/s in using partitions such that $\Delta x_i = \sqrt{gh_i}\Delta t$ with $\Delta t = 0.05$. Our main interest was the wave amplitude in the beach basin, because that is the wave amplitude that hits the shore. Without any breakwater, an incoming wave of amplitude A results in a $2A$ wave amplitude in the beach basin, so the wave amplitude values in the beach basin were scaled with a factor $2A$.

Fig. 5 shows the development and the long term behaviour of wave amplitude in the beach basin as a function of time. At first the wave hits the hard wall with amplitude $2A$ (or $A_T/2A = 1$), but as time passes this amplitude decreases by 64% in the case of destructive superposition given by Eq. (3.2), whereas in the case of constructive superposition given by Eq. (3.3) it increases up to 156%. Let us denote $\eta(L_2 + L_b, t)$ for large t as A_T and compute A_T for several values of L_b. Fig. 6 shows that $A_T/2A$ depends on L_b periodically and varies between $0.63 - 1.56$, so the transmitted amplitude A_T varies between 1.26 to 3.12 times the amplitude A of the incident waves. This confirms the formula for the safest distance Eq. (3.2), and Eq. (3.3) for the most dangerous. In the case of two-bar submerged breakwater, where each bar has the same width and height as the one-bar and separated by a distance $L_1 = \frac{\pi}{2\omega}\sqrt{gh_1}$, the values of $A_T/2A$ vary between $0.42 - 2.38$.

For a periodic submerged bar, we considered the function

$$p(x) = \begin{cases} h_+ \equiv h_1 + d, & \text{for } 0 < x < L_+, \\ h_- \equiv h_1 - d, & \text{for } L_+ < x < L_+ + L_-, \end{cases}$$

with the optimal width $L_\pm = \frac{\pi}{2\omega}\sqrt{gh_\pm}$. For computations with periodic bar, we took a bottom profile consisting of three humps and three troughs: — i.e. $h(x) = p(x) + p(x - L_+ - L_-) + p(x - 2L_+ - 2L_-)$ for $0 < x < 3(L_+ + L_-)$ and $h(x) = h_1$ elsewhere, with the hard-wall beach on the right at $x = 3(L_+ + L_-) + L_b$. For this bottom topography there are seven places where scattering takes place. Using argument similar to that in § 3, we deduce

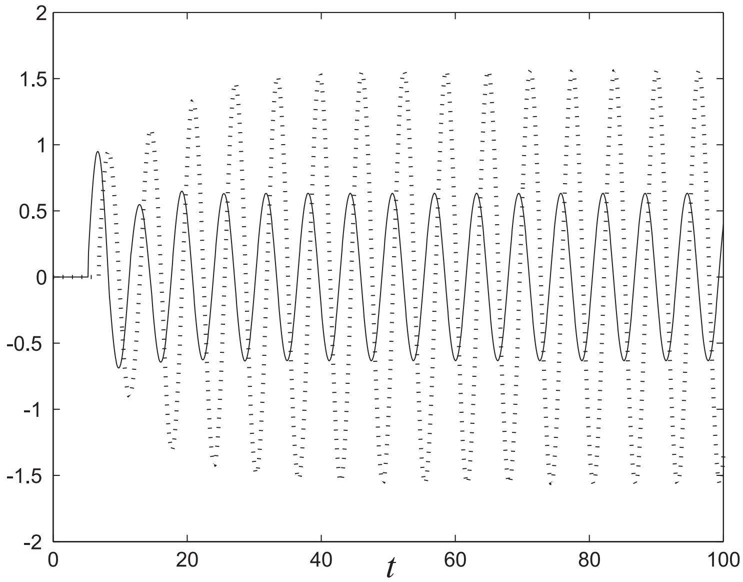

Figure 5: The curve $\eta(L_2 + L_b, t)/2A$ for $t \in [0, 100]$ with $L_b = 5\pi$ (solid line) and $L_b = 10\pi$ (dotted line).

that the phase difference between two successive right running waves in the beach basin $3(L_+ + L_-) < x < 3(L_+ + L_-) + L_b$ is also $2k_1 L_b + \pi$. Thus the formulae for the safest and the most dangerous L_b are again Eqs. (3.2) and (3.3), respectively. Using $d = 2, h_1 = 10$ we also computed the long term value A_T for several values of L_b, and the resulting curve for $A_T/2A$ is shown in Fig. 6. The values of $A_T/2A$ vary between 0.55 and 1.73.

In summary, we have analysed the safest and the most dangerous distances for three formations of submerged breakwater with optimal dimension, where all confirm the analytical formulae for the safest and the most dangerous distance of the beach. Again, it is to be expected that analogous argument and numerical implementation applies to any formation of submerged bar breakwater with optimal dimension, to provide the largest and smallest wave amplitudes in the beach basin.

4. Conclusions

The effect of a hard-wall beach on the protective function of a submerged bars breakwater has been investigated. By analysing constructive or destructive interference between successive right running waves on the beach basin, we obtained a formula for the safest and the most dangerous distances, depending on the parameters of the configuration (the bar height and the distance between bars). By applying the numerical method of characteristics to the Riemann invariant form of the shallow water equation, the long term wave interaction behaviour was simulated, and the wave amplitude in the beach basin obtained. Numerical results confirm the analytical formulae for the safest and the most dangerous distances.

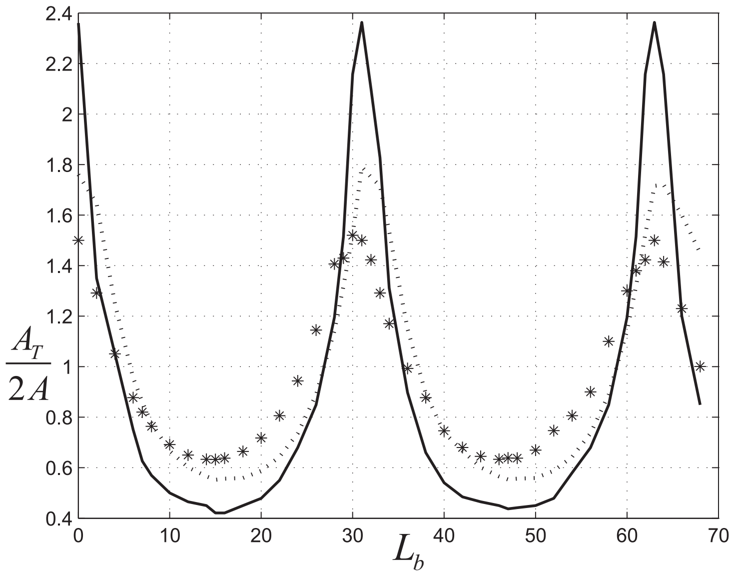

Figure 6: Curves of $A_T/2A$ with respect to L_b for one-bar (stars), two-bar (solid lines), periodic bar with three humps and troughs (dotted lines).

Acknowledgments

Our special thanks go to F. P. H. van Beckum at University of Twente for useful discussions about phase differences. The first author (SRP) acknowledges financial support from Riset KK ITB Grant No. 249/K01.7/PL/2010 and partially from Riset IA 2010 No. 1443d/K01.7/PL/2010.

References

[1] Mei, C.C., Stiassnie, M., Yue, D.K.-P., *Theory and Applications of Ocean Surface Waves*, Advanced Series on Ocean Engineering Vol. 23, World Scientific, 2004.
[2] Pudjaprasetya, S. R. & Chendra, H.D., An optimal dimension of submerged parallel bars as a wave reflector, Bull. Malays. Math. Sci. Soc. (2), **32**(1) (2009), pp. 55-62.
[3] Wiryanto, L.H., Wave propagation over a submerged bar, *ITB J. Sci.*, **42**A(2) (2010), pp. 81-90.
[4] Mattioli, F., Resonant reflection of a series of submerged breakwaters, *Il Nuovo Comento*, **13**C(5) (1990), pp. 823-833.
[5] Heathershaw A.D., Seabed-wave resonance and sandbar growth, *Nature*, **296** (1982), pp. 343-345.
[6] Davies, A.G. & Heathershaw, A.D., Surface wave propagation over sinusoidally varying topography, *J. Fluid Mech.*, **144** (1984), pp. 419-443.
[7] Yu, J. & Mei, C.C., Do longshore bars shelter the shore?, *J. Fluid Mech.* **404** (2000), pp. 251-268.
[8] Andonowati & Groesen, E. van, Similarities between optical and surface water waves, *MIHMI*, **8**(3) (2002), pp. 1-8.

[9] GISOLF, D. & VERSCHUUR, E., *The Principles of Quantitative Acoustical Imaging*, EAGE Publications, 2010.

[10] HOFFMAN, J.D., *Numerical Methods for Engineers and Scientists*, McGraw-Hill, Inc., 1992.

[11] REY, V., BELZONS, M., GUAZZELLI, E., Propagation of surface gravity waves over a retangular submerged bar, *J. Fluid Mech.*, **235** (1992), pp. 453-479.